

# High Yield Synthesis and Chemical Exfoliation of Two-Dimensional Layered Hafnium Disulphide

Harneet Kaur<sup>1,\*</sup>, Sandeep Yadav<sup>2</sup>, Avanish K. Srivastava<sup>1</sup>, Nidhi Singh<sup>1</sup>, Shyama Rath<sup>3</sup>, Jorg J Schneider<sup>2</sup>, Om P. Sinha<sup>4</sup> and Ritu Srivastava<sup>1,\*</sup>

<sup>1</sup>National Physical Laboratory, Council of Scientific and Industrial Research, Dr. K. S. Krishnan Road, New Delhi 110012, India

<sup>2</sup>Technische Universität Darmstadt, Eduard-Zintl-Institut für Anorganische und Physikalische Chemie L2 I 05 117, Alarich-Weiss-Str 12, 64287 Darmstadt, Germany.

<sup>3</sup>Department of Physics and Astrophysics, University of Delhi, Delhi 110007, India

<sup>4</sup>Amity Institute of Nanotechnology, Amity University UP, Sector 125, Noida, Uttar Pradesh 201313, India.

\*[harneet@mail.nplindia.org](mailto:harneet@mail.nplindia.org)  
[ritu@nplindia.org](mailto:ritu@nplindia.org)

## Abstract

Hafnium disulphide (HfS<sub>2</sub>) is a layered two-dimensional material of group IV transition metal dichalcogenides having potential in the field of electronic applications. However, producing its monolayers and few-layers in high yield with environmental stability is still a challenge to explore its unlocked applications. Here, for the first time we demonstrate a method to grow layered crystals of HfS<sub>2</sub> with surprisingly large interlayer spacing followed by its chemical exfoliation. Various microscopic and spectroscopic techniques reveal these as-grown crystals exfoliate into single or few layers in some minutes using solvent assisted ultrasonication method in solvents like N-Cyclohexyl-2-pyrrolidone (CHP). The exfoliated nanosheets of HfS<sub>2</sub> exhibit an indirect bandgap of 1.3 eV with high stability against ambient degradation. Further, we demonstrate that these nanosheets holds potential for electronic applications by fabricating field-effect transistors based on few layered HfS<sub>2</sub> exhibiting low-field-effect mobility of 0.95 cm<sup>2</sup>/V-s with a high current modulation ratio ( $I_{\text{on}}/I_{\text{off}}$ ) of 10<sup>4</sup> in ambient.

## Introduction

Recently, two-dimensional (2D) layered inorganic materials have flattered the research community and became the front runners in the field of material science<sup>1-3</sup>. A lot of research activity in the past few years has demonstrated the potential of these materials in the field of high speed electronics and optical detectors<sup>3-4</sup>, energy generation and storage<sup>5-6</sup>, chemical and gas sensors<sup>7-8</sup> and in bio-sensing<sup>9-10</sup>. Currently, this 2D class consists of many families, the simplest being honeycomb lattice “graphene” which is an excellent conductor<sup>11</sup> and on opposite side is “hexagonal-boron nitride (h-BN)” which is an excellent insulator<sup>12</sup>. Between these two extreme corners, there exists a wide family of 2D class called as “transition metal dichalcogenides (TMDs)” consisting of 88 members<sup>13</sup>. Depending upon the group of TMDs, it consists of metals, semiconductors and superconductors with strong covalent coupling in the monolayers and weak interlayer coupling<sup>13</sup>. The most explored group among them is VIB TMDs consisting of semiconductors like molybdenum disulphide ( $\text{MoS}_2$ )<sup>14-16</sup>. But theoretically, it has been predicted that group IVB TMDs conduct superior opto-electronics than group VIB<sup>17</sup>. Despite of this fact, very sparsely work has been conducted on group IVB TMDs.

A group of researchers recently demonstrated phototransistors based on hafnium disulphide ( $\text{HfS}_2$ ), which is a group IVB TMD, exhibiting high photosensitivity<sup>18</sup>. Even top gated transistors with  $\text{HfS}_2$  as a conducting channel material were also demonstrated, offering high current modulation ratios<sup>19-20</sup>. However, most of this recent work on  $\text{HfS}_2$  was based on micromechanical cleavage technique from its commercial available crystal<sup>18-20</sup>. There is no established method or protocol to produce  $\text{HfS}_2$  monolayers or few layers in high yield. Further, DFT calculations have predicted large interlayer interaction energy among the  $\text{HfS}_2$  layers compared to  $\text{MoS}_2$  making it difficult to exfoliate this material<sup>21</sup>. But to realize the unlocked applications of  $\text{HfS}_2$  in 2D regime, it is crucial to grow its crystal which can be

exfoliated easily using simple wet-chemical routes for its high-yield production. In past, wet chemical approaches have been proved to be very promising in producing high yield of few-layers nanosheets dispersed in solvents<sup>22-25</sup>. These methods apart from being versatile are cost-effective, simple and scalable. One such mostly used method among them for layered materials is solvent assisted ultrasonication<sup>22</sup>. Using solvents like N-methyl-2-pyrrolidone, various TMDs like MoS<sub>2</sub>, MoSe<sub>2</sub>, and WS<sub>2</sub> etc. has been exfoliated<sup>22</sup>. Even a new member of this 2D class “phosphorene” has been exfoliated using the same approach<sup>26</sup>. Further, large area electronics can be realized using these exfoliated suspensions in techniques like Langmuir-Blodgett assembly<sup>27</sup> or inkjet printing<sup>28</sup> by depositing these nanosheets on flexible substrates for next generation opto-electronics. Also, these free-standing nanosheets in the solvents can be readily mixed with proteins or organic materials to make functional hybrid structures having applications in biosensing<sup>29</sup>, organic light emitting diodes<sup>30</sup> or photovoltaic applications<sup>31</sup>.

Therefore, in this work, we demonstrate a chemical vapor transport route to produce clusters of elongated layered shiny crystals of HfS<sub>2</sub>. The as-prepared elongated crystals (named “needles”) possess a slightly extended interlayer spacing, making it easy to exfoliate it. A high yield of monolayers and few layers in solvents such as N-Cyclohexyl-2-pyrrolidone (CHP) has been achieved using solvent assisted ultrasonication method in ambient conditions. The stable dispersions of exfoliated HfS<sub>2</sub> nanosheets in CHP show the presence of an indirect bandgap of 1.3 eV and are found to be stable against surface degradation for many days unlike mechanical exfoliated flakes<sup>21</sup>. Finally, we demonstrate a bottom gate field-effect transistor (FET) with exfoliated HfS<sub>2</sub> as a conducting channel material, exhibiting a low-field-effect mobility of 0.95 cm<sup>2</sup>/V-s with SiO<sub>2</sub> as a dielectric medium. The impressive gate tunability of the drain current as well as a high current modulation on- off ratio larger than 10<sup>4</sup> allows this material to be used for opto-electronic applications.

## Results and Discussion

The HfS<sub>2</sub> crystal is grown using chemical vapor transport method. Hafnium foil and sulfur powder were used as precursors with iodine as a transporting agent. The details for the growth are discussed in detail in the method section. Various microscopic and spectroscopic techniques have been employed to confirm the morphology, crystal structure and stoichiometry of the as-prepared crystal. Figure 1a shows the as-grown crystal in the quartz ampule. The size of the crystal was 4 mm X 3 mm (Figure 1b) and was found to be made up of a bunch of small reddish-orange elongated structures in the shape of needles as seen on the walls of quartz ampule (Figure 1c). To confirm the morphology, scanning electron microscopic (SEM) was used, revealing the nesting of these needles in the crystal (Figure 1d) having length larger than hundred of microns and breadth in a few microns (Figure 1e). Energy dispersive analysis of X-rays (EDAX) confirmed the presence of “Hf” and “S” atoms with atomic percentage 1:2 (inset of Figure 1e). Further, high magnified SEM images (Figure 1f,g,h,i) confirms the presence of layered structure in each needle.

The crystal structure of HfS<sub>2</sub> is confirmed by X-ray diffraction and Raman spectroscopy. As shown in Figure 2a, the diffraction pattern from HfS<sub>2</sub> matches well with *JCPDS* card No. 28-0444 confirming its CdI<sub>2</sub>-type structure<sup>14</sup> belonging to the space group *P3m1*. Further, the high intensity peak at  $2\Theta = 14.920^\circ$  corresponding to (001) *hkl* plane with narrow full-width-at-half-maximum ( $<0.2^\circ$ ) is slightly shifted from its value  $15.132^\circ$  (inset of Figure 2a). The high intensity of this peak indicates the presence of vertical oriented growth<sup>32</sup> with high crystallinity, confirming formation of elongated crystals whereas its shift in  $2\Theta$  value changed the *d* spacing between the (001) planes from 5.85 Å to 5.93 Å. This has resulted in 1.36 % of increase in the interlayer spacing between the layers of HfS<sub>2</sub> in 1T-phase. To further confirm, Figure 2b represents the Raman spectra of a single HfS<sub>2</sub> needle with 488 nm laser excitation. The Raman modes at  $255\text{ cm}^{-1}$ ,  $318\text{ cm}^{-1}$  and  $337\text{ cm}^{-1}$  is assigned to E<sub>g</sub>, E<sub>u</sub>

(LO) and  $A_{1g}$  modes respectively<sup>33</sup> which are congruent with the 1T phase of  $HfS_2$ . The  $E_g$  and  $E_u$  (LO) modes corresponds to the in-plane vibrations whereas  $A_{1g}$  mode corresponds to out of plane vibration<sup>33</sup>. It has been reported that  $A_{1g}$  Raman mode is highly intense where as  $E_g$  and  $E_u$  (LO) modes are weak in case of  $HfS_2$ <sup>21,33</sup>. However, the enhancement of in-plane vibrations modes ( $E_g$  and  $E_u$ (LO)) in our case with suppression of out-of-plane vibrations ( $A_{1g}$ ) further suggests the change in the interlayer spacing between the multilayers of  $HfS_2$  in 1T-phase. This agrees well with the results of XRD. Also, high resolution transmission electron microscopy (HR-TEM) is employed to calculate the distance between the atomic planes. Figure 2c shows the TEM of a needle. The inset represents the change in contrast with increase in the number of layers. The atomic scale image revealed the presence of “Hf” and “S” atoms arranged in 1T-phase of  $HfS_2$  with interlayer spacing of 0.6 nm. This result is consistent with the value of  $d$  spacing for (001) plane as calculated by XRD. Therefore, formation of highly crystalline  $HfS_2$  with a slight extension in interlayer spacing is confirmed. Further, the distance between the two “Hf” atoms was calculated to be 0.3 nm which matches well the unit cell parameter of  $HfS_2$  ( $a = 0.36$  nm). A corresponding selected-area-electron diffraction pattern (SAEDP) from the needle (inset in Figure 2d) shows the presence of a set of Debye rings in reciprocal space, as displayed in Figure 2f. The SAEDP clearly reveals that the individual needles were well crystallized with the organization of atomic planes in the single crystalline nature with no evidence of structural disorder.

To cleave the atomic layers of  $HfS_2$  crystal, solvent assistant ultrasonication method was employed. The crystal was suspended in N-Cyclohexyl-2-pyrrolidone (CHP) and exposed to ultrasonic waves. These waves create cavitation bubbles, collapsing into high energy jets, resulting in the breaking of van der Waals forces in layered materials. However, it has been reported that the surface energy of the solvent used, should be similar to the energy required to avoid re-aggregation of its layers<sup>22</sup>. Since, CHP belongs to the group of amide solvents like

N-methyl-2-pyrrolidone which has been frequently used to exfoliate other 2D materials in ambient oxygen<sup>22</sup>. Therefore, this solvent was chosen to carry out the exfoliation process. The ultrasonication of the crystal in CHP yields a transparent yellow-orange dispersion as seen in the inset of Figure 3a in a time span of just a few minutes. The un-exfoliated material was removed by centrifugation at 3,000 r.p.m for 45 min to yield a suspension of few-layered HfS<sub>2</sub> sheets in CHP (see the method section for complete details). Since CHP is a high boiling point solvent which cannot be evaporated at room temperature, an additional high speed centrifugation at 13,000 r.p.m (120 min) is employed to separate out the exfoliated nanosheets of HfS<sub>2</sub> from CHP. This results in the extraction of exfoliated nanosheets by discarding the transparent CHP supernatant. The extracted sheets were suspended in toluene by mild shaking and used for further characterizations. SEM images on the drop-cast films revealed (Figure 3a) the beginning of exfoliation by breaking the elongated crystals (needles) into thin layered structures which is further confirmed by TEM (inset Figure 3a) revealing the presence of few layered HfS<sub>2</sub> sheets. As the sonication time increases, the transparency of the suspension decreases with the increase in the brightness of the suspension (inset of Figure 3b), which suggests increase in the concentration of a few-layered HfS<sub>2</sub> sheets in CHP. SEM (Figure 3b) and TEM images (inset figure 3b) confirms the presence of ultra-thin layers HfS<sub>2</sub> confirming the completion of exfoliation process within 120 min. The atomic scale TEM image (figure 3c) of an ultrathin sheet (inset of figure 3b) shows the top view of 1T phase of HfS<sub>2</sub>. A clear hexagonal lattice structure is observed without the need of Fourier transform of the image where each “Hf” atom is surrounded by six “S” atoms. Also, the interplanar spacing between the “Hf” planes i.e; 0.4 nm corresponding to (100) *hkl* plane and 0.2 nm corresponding to (101) *hkl* planes is large compared to the *d* spacing 0.32 nm for (100) *hkl* planes and 1.8 nm for (101) *hkl* planes as calculated by the XRD. However, the lattice structure appears to be intact over wide regions suggesting that HfS<sub>2</sub> can be exfoliated like

other 2D materials without introduction of defects. Figure 3d represents the SAEDP of the HfS<sub>2</sub> nanosheet (inset of figure 3b) revealing the presence of important hkl planes in reciprocal space. This confirms the high crystallinity and the preservice of pristine phase of HfS<sub>2</sub> during exfoliation. To assess the lateral dimensions of exfoliated HfS<sub>2</sub> sheets, we performed statistical FE-SEM analysis, confirming a dominating lateral size distribution associated with  $L \sim 1 \mu\text{m}$ . To further characterize the HfS<sub>2</sub> exfoliated dispersion, UV-Visible absorption spectroscopy is employed. Figure 3f shows the absorbance of HfS<sub>2</sub> as a function of sonication time. The increase in absorbance clearly suggests the increase in concentration of HfS<sub>2</sub> nanosheets in CHP solvent with the increase in sonication time. Further, the plot of  $(\alpha h\nu)^{1/2}$  versus  $h\nu$  (inset of Figure 3f) shows linearity confirming its an indirect band-gap material. The indirect bandgap as calculated from the intercept of the plot increased from 0.9 eV to 1.3 eV with the increase in sonication time suggesting indirect bandgap increases with the decrease in layer number. Our results are consistent with the DFT simulated bandgap of HfS<sub>2</sub> as recently reported by the other group<sup>21</sup>.

The structural integrity of the exfoliated sheets is confirmed by Raman spectroscopy. The Raman spectrum shown in Figure 4a represents the characteristic E<sub>g</sub>, E<sub>u</sub>(LO) and A<sub>1g</sub> phonon modes of HfS<sub>2</sub> nanosheet (inset of Figure 4a). The E<sub>g</sub> and E<sub>u</sub>(LO) modes are found to be highly intense while the A<sub>1g</sub> mode is suppressed. Since both E<sub>g</sub> and E<sub>u</sub> phonon modes corresponds to the vibrations in the basal plane while the A<sub>1g</sub> phonon mode corresponds to out of plane basal vibrations. This suggests that this enhancement of in-plane vibrations (E<sub>g</sub> and E<sub>u</sub>) is due to the extended interplanar spacing (as observed in TEM, Figure 3c) resulting in the oscillations of atoms more freely while the suppression of out-of plane vibrations (A<sub>1g</sub>) indicates a decrease in the interaction among the layers because of extended interlayer spacing (as observed in TEM, Figure 2c). Further, it has been reported that the surface of HfS<sub>2</sub> readily gets oxidized in presence of ambient oxygen increasing its thickness by 250 %

due to penetration of oxygen atoms inside the layers within a time span of 24 hours<sup>21</sup>. This significantly decreases the Raman intensity of the phonon modes<sup>21</sup>. However, we found that exfoliation in CHP provides shielding against the degradation of sheets due to ambient oxygen for several days. The Raman spectra taken after a week of ambient exposure showed the presence of highly intense  $E_g$  and  $E_u$  modes as compared to the first day in Figure 4a. Also, atomic force microscopy is a reliable tool to study the degradation of the surface. Figure 4b represents the atomic force microscopic images of  $HfS_2$  nanosheet continuously scanned for 6 days. No change in thickness or formation of any bubbles on the surface is observed. This suggests sheets exfoliated in CHP provide stability against ambient degradation.

Furthermore, we investigated the electronic applications of exfoliated  $HfS_2$  nanosheets by fabricating field-effect transistors with silicon-dioxide (230 nm) as a bottom gate dielectric. Figure 4c shows the atomic force microscopic image of the fabricated FET. A semiconducting channel is built by an  $HfS_2$  nanosheet having a thickness of 18 nm between two gold electrodes (thickness 30 nm each) acting as source and drain respectively, providing a channel length (L) of 2 microns. The channel width (W) is found to be 1.2 microns. The source electrode was grounded and the drain electrode was given a positive bias with respect to source ( $V_{DS}$ ). The back gate voltage ( $V_{BG}$ ) was applied to the doped silicon substrate. The output characteristic of the fabricated FET is shown in Figure 4d. A clear saturation of drain current ( $I_{DS}$ ) was observed corresponding to each gate bias voltage which was tuned from -2V to 10 V. Figure 4e shows the transfer characteristic of the FET. The left and right y-axis represents the linear and logarithmic scale respectively for the variation of  $I_{DS}$  with  $V_{BG}$  (x-axis) for a fixed  $V_{DS}$  of 3V. The device exhibits uni-polar n-type transport behaviour. A maximum drain current of 0.24  $\mu A/\mu m$  is obtained at a gate voltage of 20 V. The FET device exhibits a high current on-off modulation ratio larger than 10,000 at room temperature when



gate voltage is varied from 0V to 20 V. Further, low-field effect mobility was extracted from the relation:  $\mu = g_m C_g^{-1} V_{DS}^{-1} L/W$ , where  $g_m$  represents transconductance (calculated from the slope of  $I_{DS}$  versus  $V_{BG}$ ),  $C_g$  represents gate capacitance ( $\epsilon_0 \epsilon_r / d = 1.501 \times 10^{-4} \text{ F/m}^2$ ). The mobility was coming out to be  $0.95 \text{ cm}^2/\text{V-s}$ . This low value of mobility with a high on/off current modulation ratio at room temperature agrees well with the reported values of other groups<sup>19-20</sup> on micromechanical exfoliated flakes of  $\text{HfS}_2$ . Hence, solvent assisted ultrasonication method produced nanosheets of  $\text{HfS}_2$  retaining their pristine semiconducting properties as shown by the high quality mechanical exfoliated sheets.

## Conclusion

In summary, we have demonstrated a systematic route for the high yield production of  $\text{HfS}_2$  layered crystals followed by providing a simple solvent assisted ultrasonication process for their exfoliation in CHP to produce their ultra-thin layers in huge quantities. The ultra-thin nanosheets were found to retain their pristine surface without any ambient degradation for many days unlike mechanical exfoliated flakes. Further, these nanosheets were found to be as competent as other two-dimensional materials in opto-electronic applications as demonstrated by fabricating  $\text{HfS}_2$ -FET providing a high current modulation of over 10000 at room temperature. Our results open avenues for the inexpensive production of layered  $\text{HfS}_2$  in high yield to reveal the unlocked applications of this layered material.

## Methods

**Crystal Growth.** Single crystals of  $\text{HfS}_2$  were prepared by the chemical vapor transport (CVT) method. In this work, stoichiometric proportions of hafnium foil (99.9%, 0.25 mm thick, chemPUR GmbH) and sulphur powder (99.998%, Sigma Aldrich) with 5 mg iodine (99.8%, Sigma Aldrich) as a transport agent, added in an evacuated (approx.  $3 \times 10^{-3}$ ) clean quartz ampule having inner diameter 1 cm and 0.25 mm wall thickness. The ampule was

loaded in the CVD furnace (HORST GmbH) and temperature was increased to 925°C at the constant rate of 2°C/min and kept at 925 °C for 2 hours, followed by a slow cooling at the rate of 1°C/min to a temperature of 825 °C and continued the growth process for four days. After four days, furnace was cooled down to the room temperature and red metallic/orange crystals were obtained and used for characterization. X-ray diffraction (XRD), Raman spectroscopy, scanning electron microscopy (SEM), energy dispersive analysis of X-Rays (EDAX) and transmission electron microscopy (TEM) was performed using Rigaku miniFlex 600, Jobin-Yvon Horiba (HR-800Raman, 488 nm argon laser), Philips XL-30 FEG, XL30-939-2.5 CDU-LEAP-detector and Tecnai G2 F30 STWIN, TEM respectively.

**Exfoliation.** As-prepared HfS<sub>2</sub> crystals (50 mg) were dispersed in CHP (10ml, Sigma-Aldrich) and kept in a sealed vial of volume 20 ml. Further, these sealed vials were wrapped with parafilm before placing it into elmasonic TI-H bath sonicator. The dispersion was sonicated in DI water for 2 hours at 25 KHz. Temperature of DI water in ultrasonic bath was maintained at 30°C. The colour of the suspension gradually changes from light transparent yellow to dark orange-yellow in two hours, yielding a suspension of few-layers HfS<sub>2</sub> nanosheets in CHP. The suspension was centrifuged at 3000 r.p.m for 45 min in a spinwin micro centrifuge (Tarsons) to remove the un-exfoliated material and the supernatant was decanted, and subjected to UV-Visible absorption spectroscopy using Shimadzu, UV-2401. Further an additional centrifugation at a high speed of 13,000 r.p.m (120 min) is employed to suspend the exfoliated nanosheets in toluene. The supernatant resulted from this high speed centrifugation consists of transparent CHP and a precipitate containing exfoliated nanosheets of HfS<sub>2</sub>. The precipitate was extracted and mixed in toluene by mild shaking. The mixed suspension of exfoliated nanosheets in toluene was again subjected to a high speed centrifugation at 13,000 r.p.m. (30 min) to remove any traces of CHP. This process is repeated thrice and final precipitate was suspended in toluene (concentration ~0.01 mg/ml)

and used for characterizations by making films on SiO<sub>2</sub>/Si substrates and TEM grids by drop-cast method.

**FET fabrication.** The devices were fabricated on doped silicon substrates ( $\sim 3 \times 10^{17} \text{ cm}^{-3}$ ) with silicon dioxide (230 nm) as a dielectric medium with patterned gold electrodes of channel length 2 microns (OFET chip, Fraunhofer). To make the devices, large sheets of HfS<sub>2</sub> were size separated by centrifugation of the toluene suspension at a low speed of 4,000 r.p.m. for 45 min. This resulted in a precipitate consisting of larger thick sheets of HfS<sub>2</sub> which were diluted with toluene and drop-cast onto the patterned OFET chips to make devices. The devices were annealed in vacuum ( $\sim 10^{-5}$  mbar) at 120°C for six hours before room temperature measurements were taken using Keithley 4200 equipped with semiconductor characterization system (Summit 11000M, probe station). Atomic force microscopy (Pro P47 SOLVER, NT-MDT) in tapping mode was used to measure the parameters and thickness of the as-formed device.

**Characterization.** Carl Zeiss, Supra 40 VP FE-SEM was used to characterize the morphology of drop-cast films as a function of sonication time on SiO<sub>2</sub>/Si substrates at an accelerating voltage of 3 KV. The AFM images were scanned in tapping mode at a frequency of 1 Hz using Pro P47 SOLVER, NT-MDT. A Tecnai G2 F30 STWIN, TEM was used for low and high resolution imaging of exfoliated HfS<sub>2</sub> nanosheets on TEM grids at 300 KV accelerating voltage. Horiba Jobin Yvon LABRAM HR800 system coupled to an Olympus microscope with 488 nm argon-ion laser was used for Raman measurements.

**Acknowledgements.** Growth of crystal and its characterization was funded by the LOEWE project STT by the state of Hesse at Technische Universität Darmstadt. Exfoliation, its characterization and fabrication of devices were sponsored by UGC-SRF, UGC-DAE CSR-IC/CRS-77 Indore and CSIR-TAPSUN NWP-55 project.

**Author Contribution Statement.** H.K. designed, planned and executed the exfoliation experiments, fabricates devices, analyse the results and wrote the manuscript under the supervision of R.S.. S.Y. and J.J.S. grown the crystals and characterized it. A.K.S. and N.S. performed TEM characterization and FESEM characterization respectively. H.K. and S.R. performed the Raman spectroscopy measurements. J.J.S., O.P.S., S.R., and R.S. edited the manuscript. All authors reviewed the manuscript.

## References

- [1] K. S. Novoselov, D. Jiang, F. Schedin, T. J. Booth, V. V. Khotkevich, S. V. Morozov, A. K. Geim, *Proc. Natl. Acad. Sci. USA* 2005, 102, 10451-10453.
- [2] Mingsheng Xu, Tao Liang, Minmin Shi, Hongzheng Chen, *Chem. Rev.* 2013, 113(5), 3766-3798.
- [3] Gianluca Fiori, Francesco Bonaccorso, Giuseppe Lannaccone, Tomas Palacios, Daniel Neumaier, Alan Seabaugh, Sanjay K. Banerjee, Luigi Colombo, *Nat. Nanotechnol.* 2014, 9, 768-779.
- [4] F. H. L. Koppens, T. Mueller, Ph. Avouris, A. C. Ferrari, M. S. Vitiello, M. Polini, *Nat. Nanotechnol.* 2014, 9, 780-793.
- [5] Marco Bernardi, Maurizia Palummo, Jeffrey C. Grossman, *Nano lett.* 2013, 13(8), 3664-3670.
- [6] Francesco Bonaccorso, Luigi Colombo, Guihua Yu, Meryl Stoller, Valentina Tozzini, Andrea C. Ferrari, Rodney S. Ruoff, Vittorio Pellegrini, *Science* 2015, 347, 6217.
- [7] F. Schedin, A. K. Geim, S. V. Morozov, E. W. Hill, P. Blake, M. I. Katsnelson, K. S. Novoselov, *Nat. Mater.* 2007, 6, 652-655.
- [8] Yuxin Liu, Xiaochen Dong, Peng Chen, *Chem. Soc. Rev.* 2012, 41, 2283-2307.
- [9] Joonhyung Lee, Piyush Dak, Yeonsung Lee, Heekyeong Park, Woong Choi, Muhammad A. Alam, Sunkook Kim, *Sci. Rep.* 2014, 4, 7352.
- [10] Deblina Sarkar, Wei Liu, Xuejun Xie, Aaron C. Anselmo, Samir Mitragotri, Kaustav Banerjee, *ACS Nano* 2014, 8(4), 3992-4003.
- [11] A. K. Geim and K. S. Novoselov, *Nat. Mater.* 2007, 6, 183-191.
- [12] D. Pacile, J. C. Meyer, C. O. Girit, A. Zettl, *Appl. Phys. Lett.* 2008, 92, 133107.
- [13] Ruitao Lv, Joshua A. Robinson, Raymond E. Schaak, Du Sun, Yifan Sun, Thomas E. Mallouk, Mauricio Terrones, *Acc. Chem. Res.* 2015, 48(1), 56-64.
- [14] Manish Chhowalla, Hyeon Suk Shin, Goki Eda, Lain-Jong Li, Kian Ping Loh, Hua Zhang, *Nat. Chem.* 2013, 5, 263-275.
- [15] Di Xiao, Gui-Bin Liu, Wanxiang Feng, Xiaodong Xu, Wang Yao, *Phys. Rev. Lett.* 2012, 108, 196802.
- [16] Deep Jariwala, Vinod K. Sangwan, Lincoln J. Lauhon, Tobin J. Marks, Mark C. Hersam, *ACS Nano* 2014, 8(2), 1102-1120.
- [17] Wenxu Zhang, Zhishuo Huang, Wanli Zhang, Yanrong Li, *Nano Res.* 2014, 7, 1731.
- [18] Kai Xu, Zhenxing Wang, Feng Wang, Yun Huang, Fengmei Wang, Lei Yin, Chao Jiang, Jun He, *Adv. Mater.* 2015, 27, 7881-7887.

- [19] Toru Kanazawa, Tomohiro Amemiya, Atsushi Ishikawa, Vikrant Upadhyaya, Kenji Tsuruta, Takuo Tanaka, Yasuyuki Miyamoto, *Sci. Rep.* 2016, 6, 22277.
- [20] Kai Xu, Yun Huang, Bo Chen, Yang Xia, Wen Lei, Zhenxing Wang, Qisheng Wang, Feng Wang, Lei Yin, Jun He, *Small* 2016, 12, 3106-3111.
- [21] Sang Hoon Chae, Youngjo Jin, Tae Soo Kim, Dong Seob Chung, Hyunyeong Na, Honggi Nam, Hyun Kim, David J. Perello, Hye Yun Jeong, Thuc Hue Ly, and Young Hee Lee, *ACS Nano* 2016, 10, 1309-1316.
- [22] Valeria Nicolosi, Manish Chhowalla, Mercouri G. Kanatzidis, Michael S. Strano, Jonathan N. Coleman, *Science* 2013, 340, 6139.
- [23] M. Osada, T. Sasaki, *J. Mater. Chem.* 2009, 19, 2503-2511.
- [24] Z. Y. Zeng et al. *Angew. Chem. Int. Ed.* 2011, 50, 11093-11097.
- [25] M. B. Dines, *Mater. Res. Bull.* 1975, 10, 287-291.
- [26] Jack R. Brent, Nicky Savjani, Edward A. Lewis, Sarah J. Haigh, David J. Lewis, Paul O'Brien, *Chem. Commun.* 2014, 50, 13338.
- [27] Harneet Kaur, Sandeep Yadav, Avanish K. Srivastava, Nidhi Singh, Jorg J. Schneider, Om P Sinha, Ved V. Agrawal, Ritu Srivastava, *Sci. Rep.* 2016, 6, 34095.
- [28] Jiantong Li, Maziar M. Naiini, Sam Vaziri, Max C. Lemme, Mikael Ostling, *Adv. Funct. Mater.* 2014, 24, 6524-6531.
- [29] Tanyuan Wang, Ruizhi Zhu, Junqiao Zhuo, Zhiwei Zhu, Yuanhua Shao, Meixian Li, *Anal. Chem.* 2014, 86 (24), 12064-12069.
- [30] K. J. Reynolds, J. A. Barker, N. C. Greenham, R. H. Friend, G. L. Frey, *J. Appl. Phys.* 2002, 92, 7556.
- [31] Xing Gu, Wei Cui, Hai Li, Zhongwei Wu, Zhiyuan Zeng, Shuit-Tong Lee, Hua Zhang, Baoquan Sun, *Adv. Energy Mater.* 2013, 3(10), 1262-1268.
- [32] Binjie Zheng, Yuanfu Chen, Zegao Wang, Fei Qi, Zhishuo Huang, Xin Hao, Pingjian Li, Wanli Zhang, Yanrong Li, *2D Mater.* 2016, 3, 035024.
- [33] L. Roubi, C. Carlone, *Phys. Rev. B* 1988, 37, 6808.

## FIGURES

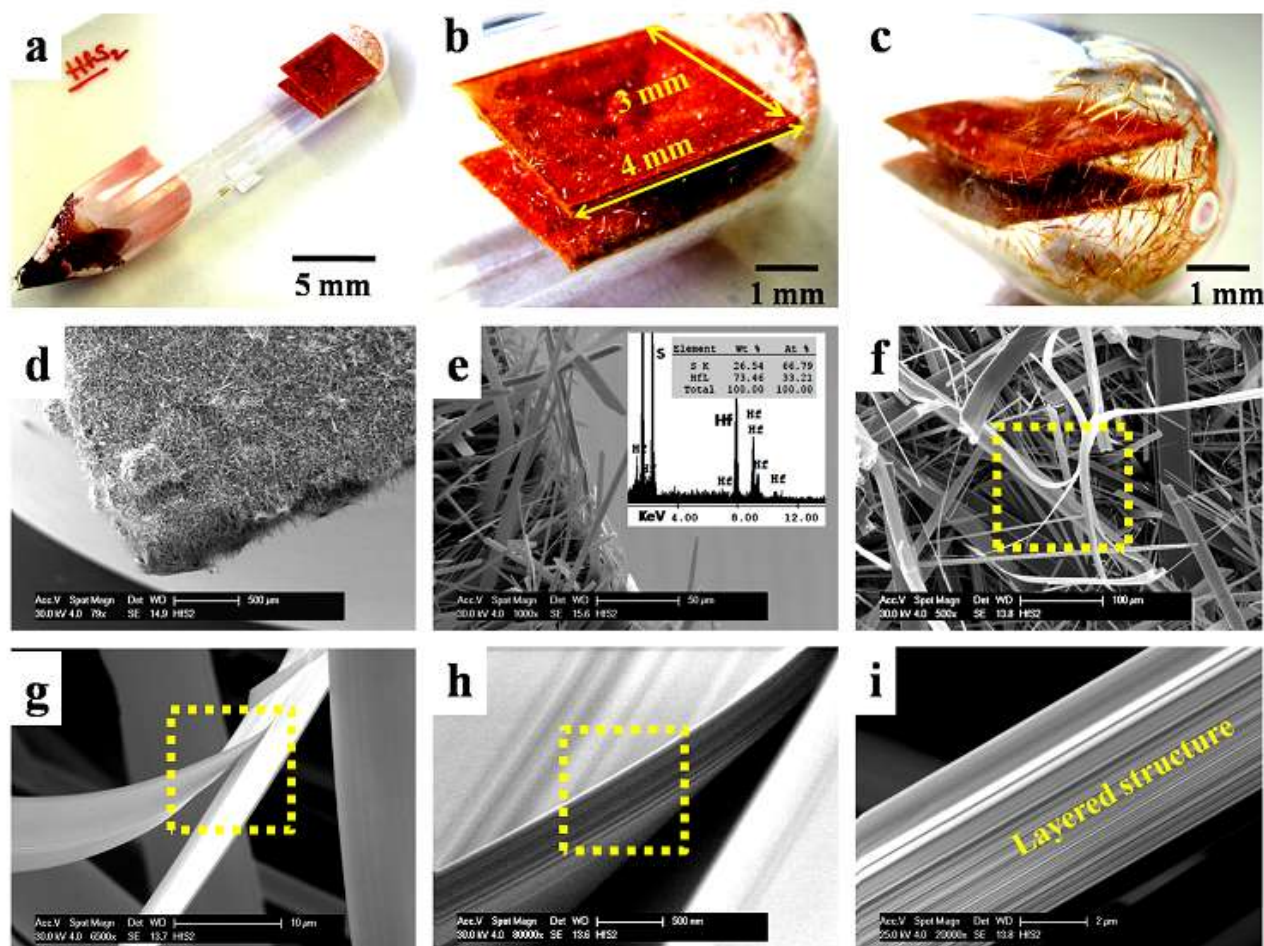


**Figure 1 shows the morphology of the as-grown crystal. (a,b,c)** Photographs of as-grown crystal in the quartz ampule. **(d,e,f)** SEM images of the crystal confirming the presence of needles shaped crystals. Inset **(e)** represents the EDAX of a needle. **(g,h,i)** SEM images confirming layered structure in each needle (yellow box shows the magnified region in the consecutive image).

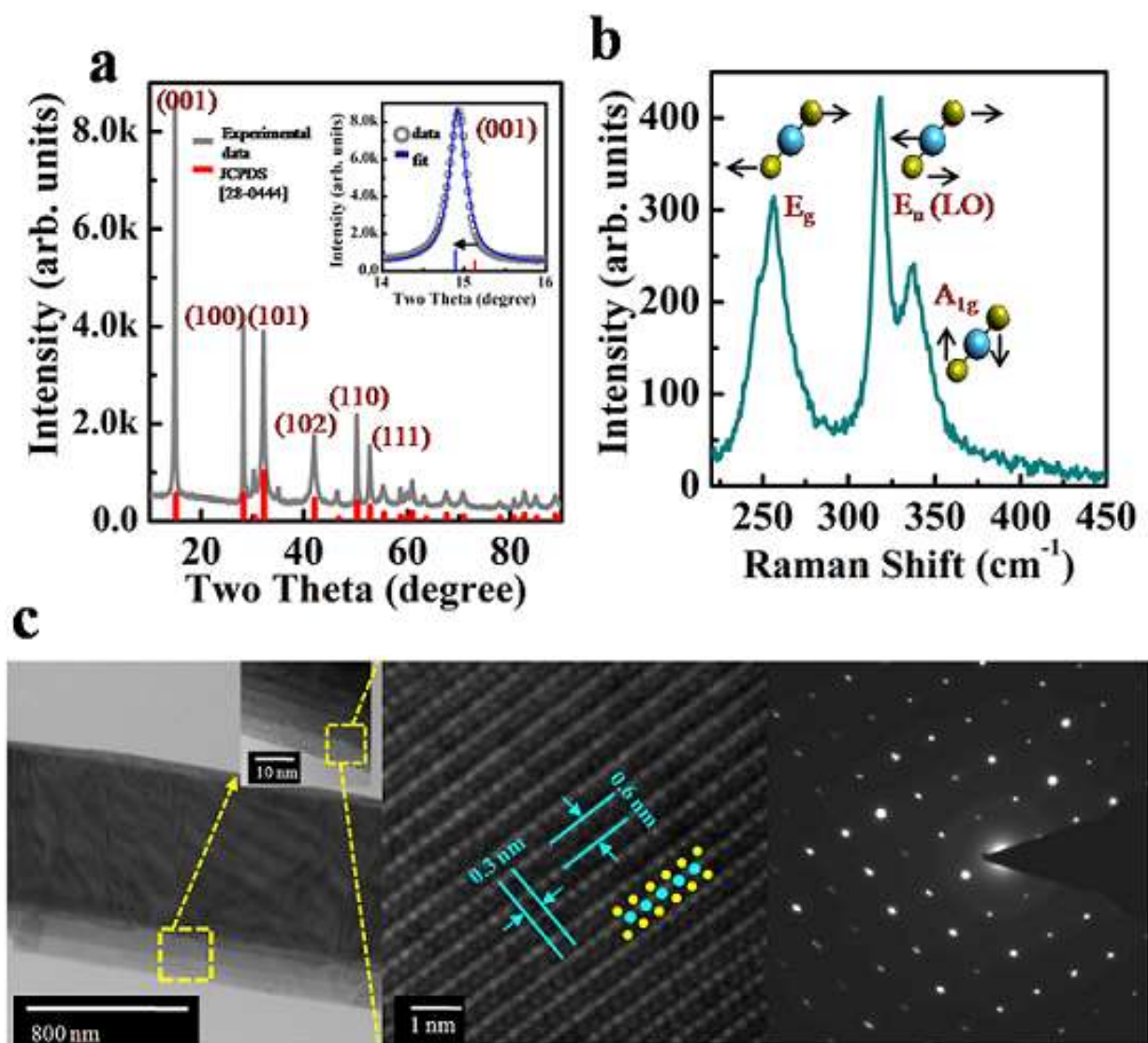


**Figure 2 shows the XRD, Raman and TEM analysis of HfS<sub>2</sub> crystal.** (a) XRD of the crystal (grey) and JCPDS card 28-0444 (red). Inset shows the shift of XRD peak for (001) hkl plane. (grey-experimental data, blue-Lorentzian fit). (b) Raman spectra of HfS<sub>2</sub> needle. (blue sphere: Hf atom, yellow sphere: S atom). (c) TEM image of HfS<sub>2</sub> needle, its magnified image (Inset), atomic scale images revealing presence of 1T-HfS<sub>2</sub> phase and selected area electron diffraction pattern (SAEDP).



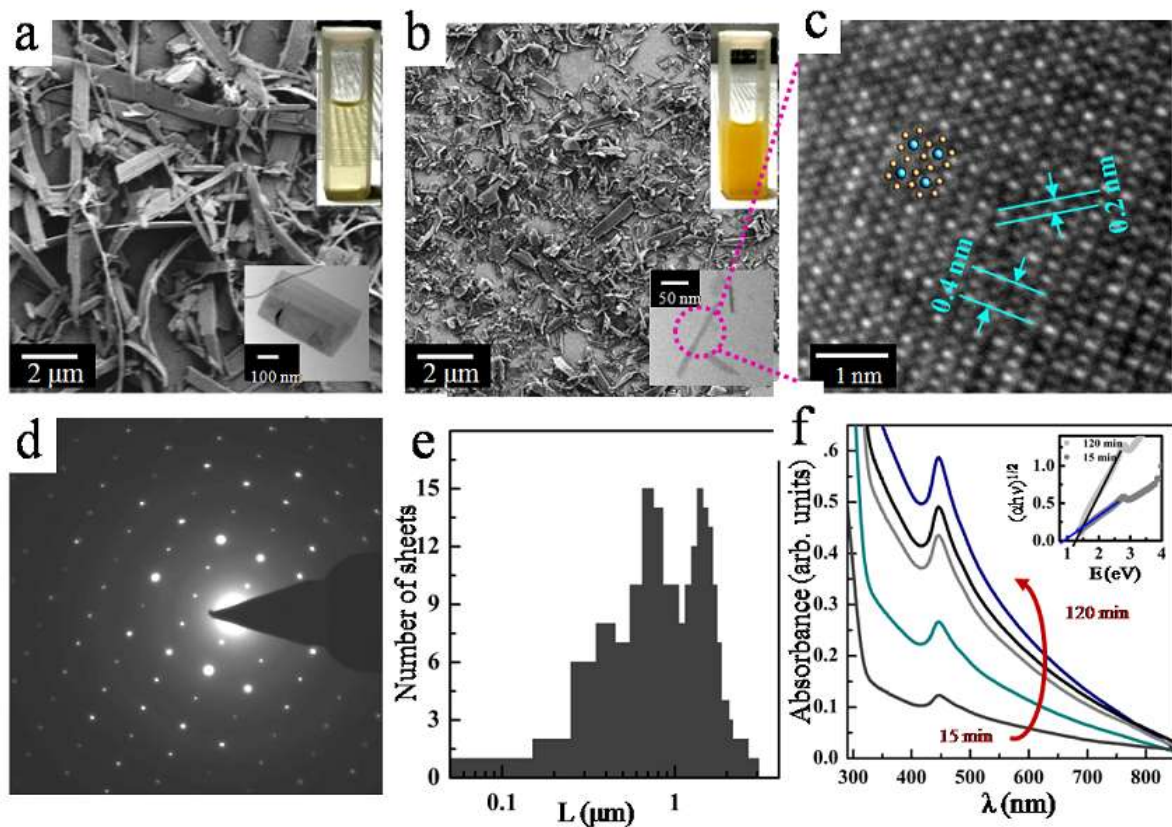


**Figure 3 shows the characterization of exfoliated HfS<sub>2</sub> nanosheets.** (a) FESEM image of the nanosheets after 15 min of ultrasonication in CHP confirming the beginning of exfoliation process. Inset represents the photograph of suspension after 15 min of exfoliation and the respective TEM image of nanosheets revealing the presence of layers. (b) FESEM image of the nanosheets after 120 min of ultrasonication in CHP resulting in the formation of ultra-thin layers of HfS<sub>2</sub> nanosheets. Inset represents the photograph of suspension after 120 min of exfoliation and the respective TEM image of ultra-thin sheets confirming the completion of exfoliation process. (c) Atomic scale HRTEM image from an ultra-thin sheet showing the top view HfS<sub>2</sub> hexagonal structure (Hf atoms: blue spheres, S atoms: orange spheres) (d) Selected-area electron diffraction pattern. (e) Statistical distribution of the size of ultra-thin nanosheets from FESEM image (sample size: 180 sheets). (f) UV- Visible absorption spectroscopy of the suspension of HfS<sub>2</sub> in CHP as a function of sonication time. Inset shows the calculated indirect-bandgap for 15 min and 120 min sonicated suspension.

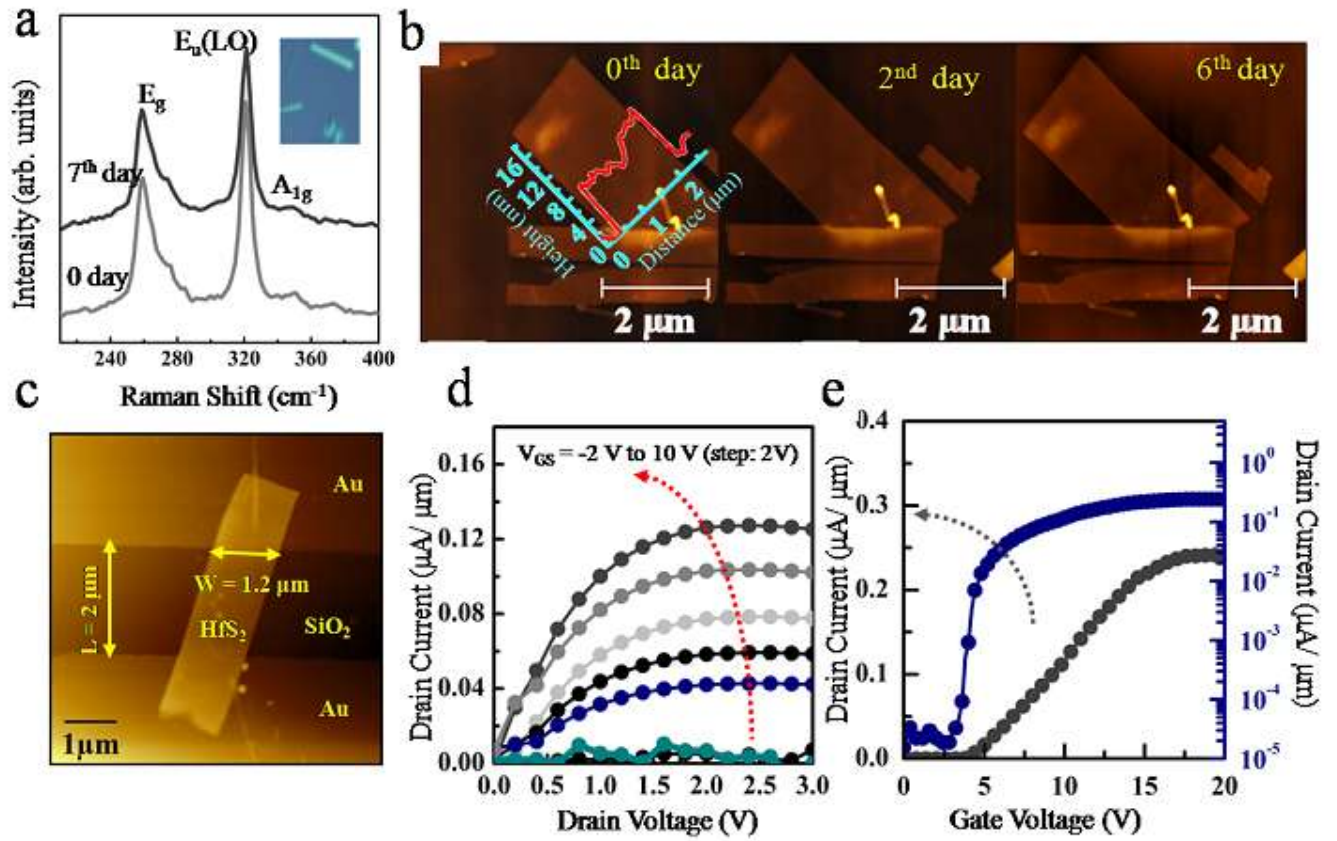


**Figure 4. Ambient stability of the nanosheets and device characteristics of HfS<sub>2</sub>-FET.** (a) Comparison of Raman spectra taken on the first day and after a week of ambient exposure confirming the stability of nanosheets. Inset shows the optical image. (b) AFM images of a few layer HfS<sub>2</sub> flake (Inset shows the height profile revealing a thickness of 8 nm) continuously scanned for a week confirming the absence of bubble formation and the sharpness of the AFM images signifying their persistence against ambient degradation. (c) AFM of the FET device (W: channel width, L: channel length, thickness of the HfS<sub>2</sub> flake: 18 nm). (d) Carrier transport by HfS<sub>2</sub> as a function of gate voltage (V<sub>GS</sub>). (e) Transfer characteristics of the HfS<sub>2</sub>-FET (left y-axis: linear scale, right y-axis: logarithmic scale).